

# Normalized mutual information is a biased measure for classification and community detection

Maximilian Jerdee,<sup>1</sup> Alec Kirkley,<sup>2,3,4</sup> and M. E. J. Newman<sup>1,5</sup>

<sup>1</sup>*Department of Physics, University of Michigan, Ann Arbor, Michigan 48109, USA*

<sup>2</sup>*Institute of Data Science, University of Hong Kong, Hong Kong*

<sup>3</sup>*Department of Urban Planning and Design, University of Hong Kong, Hong Kong*

<sup>4</sup>*Urban Systems Institute, University of Hong Kong, Hong Kong*

<sup>5</sup>*Center for the Study of Complex Systems, University of Michigan, Ann Arbor, Michigan 48109, USA*

Normalized mutual information is widely used as a similarity measure for evaluating the performance of clustering and classification algorithms. In this paper, we argue that results returned by the normalized mutual information are biased for two reasons: first, because they ignore the information content of the contingency table and, second, because their symmetric normalization introduces spurious dependence on algorithm output. We introduce a modified version of the mutual information that remedies both of these shortcomings. As a practical demonstration of the importance of using an unbiased measure, we perform extensive numerical tests on a basket of popular algorithms for network community detection and show that one's conclusions about which algorithm is best are significantly affected by the biases in the traditional mutual information.

## I. INTRODUCTION

A common task in data analysis is the comparison of two different labelings of the same set of objects. How well do demographics predict political affiliation? How accurately do blood tests predict clinical outcomes? The information theoretic measure known as mutual information is commonly applied to answer questions like these, in which an experimental or computational estimate of some kind is compared against a “ground truth.”

Mutual information [1] is a measure of how efficiently we can describe one labeling of the set of objects if we already know another labeling. Specifically, it measures how much less information it takes to communicate the first labeling if we know the second versus if we do not. As an example, mutual information is commonly used in network science to evaluate the performance of algorithms for network community detection [2]. One takes a network whose community structure is already known and applies a community detection algorithm to it to infer the communities. Then one uses mutual information to compare the output of the algorithm to the known correct communities. Algorithms that consistently achieve high mutual information scores are considered good. We will use this application as an illustrative example later in the paper.

Mutual information has a number of appealing properties as a tool for comparing labelings. It is invariant under permutations of the labels, so that, for example, two divisions of a network into communities that differ only in how the communities are labeled will be correctly identified as being the same. It also returns sensible results in cases where the number of distinct label values is not the same in the two labelings. However, the standard mutual information measure also has some significant shortcomings, and two in particular that we highlight in this paper. First, it has a bias towards labelings with too many distinct label values. For instance, a community

detection algorithm that routinely divides networks into significantly more groups than are present in the ground truth can nonetheless achieve high mutual information scores. A number of approaches for correcting this flaw have been proposed. One can apply direct penalties for incorrect numbers of groups [3] or subtract correction terms based on the average value of the mutual information over some ensemble of candidate labelings [4, 5] or on the statistics of the contingency table [6, 7]. For reasons we discuss shortly, we favor the latter approach, which leads to the measure known as the reduced mutual information.

The second drawback of the mutual information arises when the measure is normalized, as it commonly is to improve interpretability. The most popular normalization scheme creates a measure that runs between zero and one by dividing the mutual information by the arithmetic mean of the entropies of the two labelings being compared [8], although one can also normalize by the minimum, maximum, or geometric mean of the entropies. As we demonstrate in this paper, however, these normalizations introduce biases into the results by comparison with the unnormalized measure, because the normalization factor depends on the candidate labeling as well as the ground truth. This effect can be large enough to change scientific conclusions, and we provide examples of this phenomenon.

In order to avoid this latter bias, while still retaining the interpretability of a normalized mutual information measure, in this paper we propose normalizing by the entropy of the ground-truth labeling alone. This removes the source of bias but introduces an asymmetry in the normalization. At first sight this asymmetry might seem undesirable, and previous authors have gone to some lengths to avoid it. Here, however, we argue that it is not only justified but even desirable, for several reasons. First, many of the classification problems we consider are unaffected by the asymmetry, since they involve the comparison of one or more candidate labelings

against a single, unchanging ground truth. Moreover, by contrast with the multitude of possible symmetric normalizations, the asymmetric measure we propose is the unique unbiased way to normalize the mutual information such that a perfect match receives a score of 1.

But more broadly, one can argue that an asymmetric measure can be more informative than the conventional symmetric one. Consider for instance the common situation where one labeling is a fine-grained version of the other. We might for example label individuals by the country they live in on the one hand and by the town or city on the other. Then the detailed labeling tells us everything there is to know about the coarse-grained one, but the reverse is not true: telling you the city fixes the country, but not *vice versa*. Thus one could argue that the mutual information between the two *should* be asymmetric even before normalization—labeling A contains more information about labeling B than B does about A—and this type of asymmetry will be a key feature of the measures we study.

Both drawbacks of the standard mutual information—bias towards too many groups and dependence of the normalization on the candidate labeling—can be addressed simultaneously by using an asymmetric normalized reduced mutual information as defined in this paper. In support of this approach we present an extensive comparison of the performance of this and other variants of the mutual information in network community detection tasks, generating a large number of random test networks with known community structure and a variety of structural parameters, and then attempting to recover the communities using popular community detection algorithms. Within this framework, we find that conclusions about which algorithms perform best are significantly impacted by the choice of mutual information measure, and specifically that traditional measures erroneously favor algorithms that find too many communities, but our proposed measure does not. Code implementing our measure may be found at [https://github.com/maxjerdee/reduced\\_mutual\\_information](https://github.com/maxjerdee/reduced_mutual_information).

## II. MUTUAL INFORMATION

Mutual information can be thought of in terms of the amount of information it takes to transmit a labeling from one person to another. In general, if we have a set of  $N$  possible values for a quantity, such as possible labelings of a set of objects, then one can communicate a single one of them to a receiver by assigning each value a unique binary string and then transmitting the appropriate string. The minimum number of bits needed to do this is

$$H = \lceil \log_2 N \rceil \simeq \log_2 N \propto \ln N. \quad (1)$$

Conventionally one uses base-2 logarithms in this context, which gives  $H$  units of bits, but we use natural logarithms in this paper, since they are more convenient

for our purposes. The only difference is an overall factor of  $\ln 2$ , which will have no effect on our conclusions. Henceforth, all logarithms should be read as natural logs.

Suppose that we have a labeling or division of  $n$  objects into  $q$  groups, which we represent as a vector of  $n$  integer elements, each with value in the range  $1 \dots q$ . We assume there to be a ground-truth labeling, which we denote  $g$ , and a candidate labeling for comparison  $c$ , generated for instance by some sort of algorithm. The mutual information  $I(c; g)$  between the two is the amount of information that can be saved when transmitting the truth  $g$  if the receiver already knows the candidate  $c$ . We can write this information as the total entropy of  $g$  minus the conditional entropy of  $g$  given  $c$ :

$$I(c; g) = H(g) - H(g|c). \quad (2)$$

Loosely, we say that  $I(c; g)$  measures “how much  $c$  tells us about  $g$ .”

We now write down expressions for both entropies in (2), but there are some subtleties involved in doing so, because the expressions depend on how the transmitted information is encoded and also because achieving correct results requires us to carefully retain some terms that are often neglected. Our presentation follows that of [7]. First consider  $H(g)$ , which represents the information required to transmit the ground truth on its own. The transmission process has three steps. We first transmit the number of groups  $q_g$  in the labeling, followed by a vector  $n^{(g)}$  with  $q_g$  elements  $n_s^{(g)}$  equal to the number of objects in each group. Third, we transmit our final labeling  $g$ . If we apply Eq. (1) to calculate the cost of the first step, since the maximum possible value of  $q_g$  is  $n$ , transmitting any particular value requires information  $H(q_g) = \log n$ . Likewise for the third step, given  $n^{(g)}$ , there are  $n! / \prod_s n_s^{(g)}!$  labelings  $g$  that have the correct group sizes, so the amount of information needed to identify a particular labeling uniquely is

$$H(g|n^{(g)}) = \log \frac{n!}{\prod_s n_s^{(g)}!}. \quad (3)$$

The middle step, transmission of the group sizes, is more delicate: here some optimization is possible that allows us to achieve a better measure of information content. Generally when transmitting a sequence of  $n$  values with unequal probabilities such that value  $r$  occurs  $n_r$  times, the information cost is given by the generalization of Eq. (3) thus:

$$\begin{aligned} \log \frac{n!}{\prod_r n_r!} &\simeq n \log n - n - \sum_r (n_r \log n_r - n_r) \\ &= - \sum_r n_r \log p_r, \end{aligned} \quad (4)$$

where  $p_r = n_r/n$  is the probability of value  $r$  and we have approximated the factorials using Stirling’s formula. Equation 4 tells us that the information cost to transmit

the value  $r$  is simply  $-\log p_r$ . If the  $N$  possible values are equally likely to appear and  $p_r = 1/N$ , we recover the information cost of Eq. (1), but if they are not we can take advantage of that fact to create more efficient encodings.

The transmission of  $n^{(g)}$  benefits from such an efficient encoding. We do not in general know the distribution of the elements of  $n^{(g)}$ , but we know they that may be—and often are—heterogeneous. As shown in [7], an effective approach is to assume a Dirichlet-multinomial distribution with concentration parameter  $\alpha_g > 0$

$$P(n^{(g)}|q_g, \alpha_g) = \left( \frac{n + q_g \alpha_g - 1}{q_g \alpha_g - 1} \right)^{-1} \prod_{r=1}^{q_g} \binom{n_r^{(g)} + \alpha_g - 1}{\alpha_g - 1}, \quad (5)$$

where for non-integer  $\alpha_g$  we generalize the binomial coefficient in the obvious way:

$$\binom{n}{k} = \frac{\Gamma(n+1)}{\Gamma(k+1)\Gamma(n-k+1)}, \quad (6)$$

with  $\Gamma(x)$  being the standard gamma function. If  $\alpha_g = 1$ , the Dirichlet-multinomial distribution is uniform over all  $q_g$ -vectors  $n^{(g)}$  of non-negative integers that sum to  $n$ . If  $0 < \alpha_g < 1$  the distribution favors vectors with more extreme elements, while for  $\alpha_g > 1$  it favors vectors with more homogeneous elements. With this choice the resulting information cost to transmit  $n^{(g)}$  is

$$H(n^{(g)}|q_g, \alpha_g) = -\log P(n^{(g)}|q_g, \alpha_g) = \log \left( \frac{n + q_g \alpha_g - 1}{q_g \alpha_g - 1} \right) - \sum_{r=1}^{q_g} \log \binom{n_r^{(g)} + \alpha_g - 1}{\alpha_g - 1}. \quad (7)$$

The optimal encoding for transmitting  $n^{(g)}$  within the Dirichlet-multinomial family is given by the minimum of this expression with respect to  $\alpha_g$ , which is also equivalent to simply maximizing  $P(n^{(g)}|\alpha_g)$ , i.e., to finding the maximum-likelihood value of  $\alpha_g$ . Note that we omit the cost of transmitting the parameter  $\alpha_g$  itself since it will ultimately cancel out of the expression for the mutual information as described in [7].

The total cost to transmit  $g$  is now equal to the sum of the individual costs of the three steps, thus:

$$\begin{aligned} H(g) &= H(q_g) + H(n^{(g)}|q_g, \alpha_g) + H(g|n^{(g)}) \\ &= \log n + \log \frac{n!}{\prod_s n_s^{(g)}!} \\ &\quad + \log \left( \frac{n + q_g \alpha_g - 1}{q_g \alpha_g - 1} \right) - \sum_{r=1}^{q_g} \log \binom{n_r^{(g)} + \alpha_g - 1}{\alpha_g - 1} \end{aligned} \quad (8)$$

This three-part encoding scheme is not the only one that can be applied to this problem, but it is an efficient one in the common case of a relatively small number of groups  $q_g \ll n$  with potentially unequal sizes, and it reduces to the conventional expression for  $H(g)$  when subleading terms are neglected. It is an important part of our

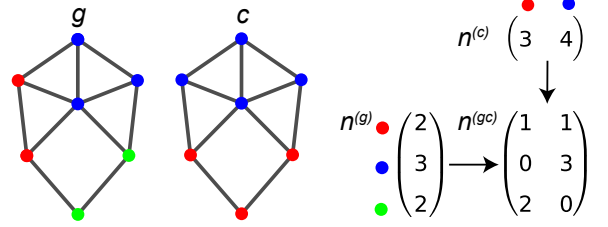


FIG. 1. An example of a contingency table for two colorings of the same network, one with three colors and one with two. The entries in the  $3 \times 2$  contingency table  $n^{(gc)}$  count the number of nodes that have each combination of colors. The row and column sums  $n^{(g)}$  and  $n^{(c)}$  of the contingency table count the number of nodes with each color in the two colorings. Note that, although we illustrate the contingency table with an application to a network, the table itself is independent of the network structure.

argument here, however, that the subleading terms be retained and carried through to the calculation of the mutual information.

For the calculation of  $H(g|c)$ , the second term in Eq. (2), we use a similar three-part encoding, but one that takes advantage of the receiver's knowledge of  $c$  when communicating  $g$ . We first communicate  $q_g$  as before, at the same information cost of  $H(q_g) = \log n$ . In place of the vector  $n^{(g)}$  we then communicate a *contingency table*  $n^{(gc)}$ , a matrix with elements  $n_{rs}^{(gc)}$  equal to the number of objects that simultaneously belong to group  $r$  in the candidate labeling  $c$  and group  $s$  in the ground truth  $g$ . Figure 1 shows an example of a contingency table for two labelings of the nodes in a small network.

Our process for transmitting the contingency table is analogous to the one we use for transmitting  $n^{(g)}$ . Since the labeling  $c$  is known, the column sums  $n^{(c)}$  of the contingency table are known as well, and we assume each column to be drawn from a Dirichlet-multinomial distribution with the appropriate sum. We use the same concentration parameter  $\alpha_{g|c}$  for every column, but the columns are otherwise independent. If we denote column  $s$  by  $n_s^{(gc)}$ , then the information cost to transmit the entire contingency table is

$$\begin{aligned} H(n^{(gc)}|n^{(c)}, q_g, \alpha_{g|c}) &= \sum_{s=1}^{q_c} H(n_s^{(gc)}|n_s^{(c)}, q_g, \alpha_{g|c}) \\ &= \sum_{s=1}^{q_c} \left[ \log \binom{n_s^{(c)} + q_g \alpha_{g|c} - 1}{q_g \alpha_{g|c} - 1} \right. \\ &\quad \left. - \sum_{r=1}^{q_g} \log \binom{n_{rs}^{(gc)} + \alpha_{g|c} - 1}{\alpha_{g|c} - 1} \right]. \end{aligned} \quad (9)$$

This formulation allows for very efficient transmission of the contingency table under commonly occurring conditions. Consider for instance the special (but not implausible) case where  $g = c$ , so that  $n^{(gc)}$  is diagonal. In

this case the optimal concentration parameter is  $\alpha_{g|c} = 0$ , which restricts the possible contingency tables to those for which each column  $n_{\cdot s}^{(gc)}$  has exactly one nonzero entry. Given that we know the column sums, this leaves only the positions of the nonzero entries within each column to be transmitted, which results in near-optimal performance, a decisive improvement over previous reductions of the mutual information [7]. Most practical applications will not have  $c = g$  precisely, but the two labelings are often similar and similarly impressive improvements in performance can be realized in such cases as well.

Finally, having transmitted the contingency table, it remains only to transmit the ground-truth labeling itself, where we need consider only those labelings consistent with the contingency table, given the known candidate labeling  $c$ . The number of such labelings is  $\prod_r n_r^{(c)}! / \prod_{rs} n_{rs}^{(gc)}!$ , so the information needed to uniquely identify one of them is

$$H(g|n^{(gc)}, c) = \log \frac{\prod_r n_r^{(c)}!}{\prod_{rs} n_{rs}^{(gc)}!}. \quad (10)$$

In typical applications the number of labelings compatible with the contingency table is much smaller than the total number of labelings, and hence this encoding substantially reduces the amount of information needed to transmit the ground truth. It is not the only encoding possible, but it is an efficient one in practice and it is the one upon which the conventional mutual information is based.

Collecting all our terms, the total conditional information can now be written

$$H(g|c) = H(q_g) + H(n^{(gc)}|n^{(c)}, q_g, \alpha_{g|c}) + H(g|n^{(cg)}, c). \quad (11)$$

And substituting (8) and (11) into Eq. (2), we get a complete expression for the mutual information

$$\begin{aligned} I(c; g) &= H(g) - H(g|c) \\ &= \log \frac{n! \prod_{rs} n_{rs}^{(gc)}!}{\prod_r n_r^{(c)}! \prod_s n_s^{(g)}!} + \log \binom{n + q_g \alpha_g - 1}{q_g \alpha_g - 1} \\ &\quad - \sum_{r=1}^{q_g} \log \binom{n_r^{(g)} + \alpha_g - 1}{\alpha_g - 1} \\ &\quad - \sum_{s=1}^{q_c} \log \binom{n_s^{(c)} + q_g \alpha_{g|c} - 1}{q_g \alpha_{g|c} - 1} \\ &\quad + \sum_{r=1}^{q_g} \sum_{s=1}^{q_c} \log \binom{n_{rs}^{(gc)} + \alpha_{g|c} - 1}{\alpha_{g|c} + 1}. \end{aligned} \quad (12)$$

In most treatments, only the first of these terms is retained, since the others are subdominant and often small [6, 7]. When all the terms are retained, however, the quantity (12) is known as the *reduced mutual information* and there are good reasons to use this full expression in certain circumstances, a point that we investigate in Section II A.

If we follow convention, however, and keep only the leading term, then we arrive at the traditional mutual information, which we denote  $I_0$ :

$$I_0(c; g) = \log \frac{n! \prod_{rs} n_{rs}^{(gc)}!}{\prod_r n_r^{(c)}! \prod_s n_s^{(g)}!}. \quad (13)$$

For later convenience, we also define entropies  $H_0$  for the individual labelings ignoring subdominant terms, which can be thought of as the mutual information between the labelings and themselves:

$$H_0(c) = I_0(c; c) = \log \frac{n!}{\prod_r n_r^{(c)}!}, \quad (14)$$

$$H_0(g) = I_0(g; g) = \log \frac{n!}{\prod_s n_s^{(g)}!}. \quad (15)$$

Note that these differ from the entropy of Eq. (8), which includes subdominant terms. Trivially (14) and (15) provide upper bounds on the mutual information, while zero is a lower bound, so

$$0 \leq I_0(c; g) \leq H_0(c), H_0(g). \quad (16)$$

These bounds will be useful shortly.

A common further step is to approximate the mutual information of Eq. (13) using Stirling's approximation in the form

$$\log n! = n \log n - n + O(\log(n)), \quad (17)$$

which gives

$$I_0(c; g) = n \sum_{rs} p_{rs}^{(gc)} \log \frac{p_{rs}^{(gc)}}{p_r^{(c)} p_s^{(g)}} + O(\log n), \quad (18)$$

where

$$p_{rs}^{(gc)} = \frac{n_{rs}^{(gc)}}{n}, \quad p_r^{(c)} = \frac{n_r^{(c)}}{n}, \quad p_s^{(g)} = \frac{n_s^{(g)}}{n}, \quad (19)$$

and we adopt the convention that  $0 \log 0 = 0$ . Equation (18) is often used as the definition of the mutual information, although technically it is only an approximation, albeit one that is asymptotically correct in the limit of large  $n$ . (It can also be derived by considering the information cost to transmit the true label of a single object, selected at random, with and without knowledge of the corresponding candidate label.)

## A. Reduced mutual information

Equation (13) defines the standard mutual information. In this paper we explore variant definitions that can perform better at the clustering tasks we consider. A number of variants have been proposed, of which the simplest in the context of the current presentation is the reduced mutual information  $I(c; g)$  of Eq. (12), which is

simply the value of the mutual information when one does not neglect the subleading information cost of transmitting the group sizes and the contingency table.

To understand the importance of the subleading terms let us explore how things can go wrong if we neglect them. To take an extreme example, suppose an algorithm simply places every object in a group of its own, which corresponds to the candidate labeling  $c = (1, \dots, n)$ . No matter what the ground truth is, this choice of  $c$  clearly contains no information about it whatsoever, so we might expect the mutual information to be zero. This, however, is not what we find. The contingency table in this case is

$$n_{rs}^{(gc)} = \begin{cases} 1 & \text{if } g_r = s, \\ 0 & \text{otherwise,} \end{cases} \quad (20)$$

so the conventional mutual information of Eq. (13) is

$$I_0(c; g) = \log \frac{n!}{\prod_s n_s^{(g)}!} = H_0(g). \quad (21)$$

This answer is not merely wrong; it is maximally so. The mutual information should take its minimum value of zero, but instead it takes the value  $H_0(g)$ , which is the maximum possible since  $H_0(g)$  is an upper bound as we have said. The reason for this result is that in this case the contingency table itself uniquely defines  $g$ , so neglecting it puts the mutual information in error by an amount equal to the complete information cost of the ground truth. If we include the subleading terms on the other hand, this erroneous behavior disappears. Assuming for simplicity that the ground-truth groups are of equal size, the optimal concentration parameters are  $\alpha_{g|c} = 0$  and  $\alpha_g = \infty$ , and the reduced mutual information of Eq. (12) becomes

$$\begin{aligned} I(c; g) &= I_0(c; g) - \log \left[ \frac{n!}{\prod_r n_r!} (1/q_g)^n \right] - n \log q_g \\ &= 0. \end{aligned} \quad (22)$$

which is the correct answer.

A related shortcoming of the standard mutual information is that for finite  $n$  a *random* labeling  $c$  will have positive mutual information with respect to any ground truth in expectation: because mutual information is non-negative, fluctuations due to randomness in finite systems will produce non-negative values only and hence their average will in general be positive [4, 9]. This seems counterintuitive: we would expect the average value for a random labeling to be zero.

We can rectify this issue by using another variant of the mutual information, which subtracts off the expected value of the measure, thereby making the average zero by definition. To do this we must first decide how a random labeling is to be defined—over what distribution of candidate labelings are we averaging? The conventional choice is to take the uniform distribution over labelings that share the same group sizes  $n^{(c)}$  as the actual candidate  $c$ . This yields the *adjusted mutual information* of

Vinh *et al.* [4]:

$$I_A(c; g) = I_0(c; g) - \langle I_0(c; g) \rangle_{\{c|n^{(c)}\}}, \quad (23)$$

where the expectation is over the relevant ensemble.

This measure can also be treated within the information-cost framework of the present paper, as described in [6]. There it is shown that the subtracted term  $\langle I_0(c; g) \rangle_{\{c|n^{(c)}\}}$  is precisely equal to the average cost of transmitting the contingency table when labelings are drawn from the uniform distribution. Thus, one can view the adjusted mutual information as a reduced measure, but differing from the one proposed in this paper in two ways. First, the correction term counts the cost of transmitting the contingency table but not the cost of transmitting the counts  $n^{(g)}$ , as described in Section II. This, however, is only a minor concern—the latter is usually much smaller than the former and its neglect introduces only a small error in most cases.

The second difference is more serious and revolves around the choice to draw labelings uniformly from those with given  $n^{(c)}$ . As discussed in [6], this distribution heavily favors contingency tables with relatively uniform entries, simply because there are many more labelings that correspond to uniform tables than to non-uniform ones. Real contingency tables, on the other hand, are often highly non-uniform, since many applications of the mutual information focus on labelings that are somewhat similar to the ground truth (producing a non-uniform table). In such cases, the average used in the adjusted mutual information puts most of its weight on configurations that are very different from those that occur in reality, making it a poor representation of true information costs. The measure proposed in this paper, by contrast, deliberately allows for non-uniform tables by drawing them from a Dirichlet-multinomial distribution and we argue that this is a strong reason to favor it over the adjusted mutual information. In addition it is also derived naturally from a fully information-theoretic argument, by contrast with the more *ad hoc* derivation of the adjusted mutual information. Notwithstanding, in Section III we give results using both reduced and adjusted mutual information, and find fairly similar outcomes in the two cases.

## B. Normalization of the mutual information

A fundamental difficulty with mutual information as a measure of similarity is that its range of values depends on the particular application, which makes it difficult to say when a value is large or small. Is a mutual information of 10 a large value? Sometimes it is and sometimes it isn't, depending on the context. To get around this problem one commonly normalizes the mutual information so that it takes a maximum value of 1 when the candidate labeling agrees exactly with the ground truth. There are a number of ways this can be achieved but, as we show

here, they are not all equal. In particular, some, including the most popularly used normalization, can result in biased results and should, in our opinion, be avoided. In its place, we propose an alternative, unbiased normalized measure.

The most popular normalized measure, commonly referred to simply as the “normalized mutual information,” uses the plain mutual information  $I_0(c; g)$  as a base measure and normalizes it thus:

$$\begin{aligned} \text{NMI}_0^{(S)}(c; g) &= \frac{I_0(c; g)}{\frac{1}{2}[H_0(c) + H_0(g)]} \\ &= \frac{I_0(c; g) + I_0(g; c)}{I_0(c; c) + I_0(g; g)}. \end{aligned} \quad (24)$$

This measure has a number of desirable features. Because of the inequalities in (16), its value falls strictly between zero and one. And since both the base measure and the normalization are symmetric under interchange of  $c$  and  $g$ , the normalized measure also retains this symmetry (hence the superscript “(S),” for symmetric).

Equation (24) is not the only normalization that achieves these goals. Equation (16) implies that

$$I_0(c; g) \leq \min(I_0(c; c), I_0(g; g)) \quad (25)$$

$$\leq \sqrt{I_0(c; c)I_0(g; g)} \quad (26)$$

$$\leq \max(I_0(c; c), I_0(g; g)), \quad (27)$$

which gives us three more options for a symmetric denominator in the normalized measure. The arithmetic mean in Eq. (24), however, sees the most use by far [10–13].

We can extend the notion of symmetric normalization to any other base measure of mutual information  $I_X(c; g)$  by writing

$$\text{NMI}_X^{(S)}(c; g) = \frac{I_X(c; g) + I_X(g; c)}{I_X(c; c) + I_X(g; g)}. \quad (28)$$

All such measures, however, including the standard measure of Eq. (24), share a crucial shortcoming, namely that the normalization depends on the candidate labeling  $c$  and hence that the normalized measure can prefer a different candidate labeling to the base measure purely because of the normalization. Figure 2 shows an example of how this can occur. Two candidate labelings  $c_A$  and  $c_B$  are considered for the same ground truth  $g$ . Under the unnormalized mutual information of Eq. (13), candidate A receives a higher score than candidate B, but under the normalized measure of Eq. (24) the reverse is true. This behavior is due to the difference in entropy between the two candidate divisions, the one on the right having larger entropy than the one on the left, which increases its normalization factor and correspondingly decreases the normalized mutual information.

We argue that the unnormalized measure is more correct on this question, having a direct justification in terms of information theory. The purpose of the normalization is purely to map the values of the measure

onto a convenient numerical interval, and should not change outcomes as it does here. Moreover, different symmetric normalizations can produce different results. For instance, if one normalizes by  $\max(I_0(c; c), I_0(g; g))$  in Fig. 2 then candidate  $c_A$  is favored in all cases.

These issues are unavoidable when using a symmetric normalization scheme. In any such scheme the normalization must depend on both  $c$  and  $g$  and hence can vary with the candidate labeling. However, if we drop the requirement of symmetry then we can normalize in a straightforward way that avoids these issues. We define the *asymmetric normalization* of any base measure  $I_X$  as

$$\text{NMI}_X^{(A)}(c; g) = \frac{I_X(c; g)}{I_X(g; g)}. \quad (29)$$

This definition still gives  $I_X^{(A)}(g; g) = 1$ , but now the normalization factor in the denominator has no effect on choices between candidate labelings, since it is independent of  $c$ . In fact, Eq. (29) is the only way to normalize such that  $I_X^{(A)}(g; g) = 1$  while simultaneously ensuring that the preferred candidate is always the same as for the base measure. Thus this measure also removes any ambiguity about how one should perform the normalization. Loosely, this asymmetrically normalized mutual information measures “how much  $c$  tells us about  $g$  as a fraction of all there is to know about  $g$ .”

The amount of bias inherent in the symmetrically normalized measure when compared with asymmetric one can be quantified by the ratio between the two:

$$\begin{aligned} \frac{\text{NMI}_X^{(S)}(c; g)}{\text{NMI}_X^{(A)}(c; g)} &= \frac{[I_X(c; g) + I_X(g; c)]/[I_X(c; c) + I_X(g; g)]}{I_X(c; g)/I_X(g; g)} \\ &= \frac{1 + I_X(g; c)/I_X(c; g)}{1 + I_X(c; c)/I_X(g; g)}. \end{aligned} \quad (30)$$

If the base measure  $I_X$  is itself symmetric (which it is, either exactly or approximately, for all the measures we consider), then this simplifies further to

$$\frac{\text{NMI}_X^{(S)}(c; g)}{\text{NMI}_X^{(A)}(c; g)} = \frac{H(g)}{\frac{1}{2}[H(g) + H(c)]}. \quad (31)$$

Note how this expression results in a particular bias against complex candidate labelings  $c$  that have higher entropy  $H(c)$  than the ground truth. Traditional mutual information measures are particularly problematic when the candidate is a *refinement* of the ground truth, meaning the candidate groups are subsets of the ground-truth groups. The example given in Section II A, in which the candidate labeling puts every node in a group on its own, is an extreme instance of this. Equation (31) shows that, to some extent, the traditional symmetric normalization corrects this issue: a candidate  $c$  that takes the form of a refinement of  $g$  will have  $H(c) > H(g)$  and hence the normalized mutual information will be penalized.

We argue, however, that this is not the best way to address the problem and that the correct approach is

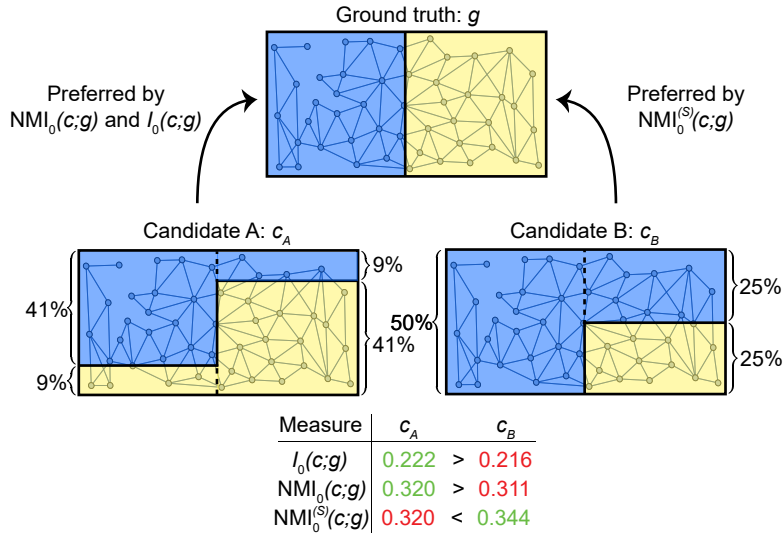


FIG. 2. An example of how normalization can impact which labeling is preferred by a mutual information measure. For the ground-truth labeling  $g$  (top), the standard unnormalized mutual information  $I_0(c, g)$  of Eq. (18) gives different scores to the two candidate labelings  $c_A$  and  $c_B$ , the former receiving a higher score than the latter. By definition, the asymmetrically normalized mutual information will always agree with the unnormalized measure, but the symmetrically normalized measure may not, as is the case here: in this example the symmetric measure scores candidate  $c_B$  higher. Note that the network itself plays no role here—it is included only as a visual aid.

instead to use the reduced mutual information. The reduced mutual information also penalizes such cases, but it does so in a more principled manner that directly addresses the root cause of the problem, rather than merely penalizing complex candidate labelings in an *ad hoc* manner as a side-effect of normalization. We will see examples of this in Section III, where we apply both measures to community detection in networks and find that, although the symmetrically normalized traditional measure is biased, it is in some cases fortuitously biased in the right direction, although it is still problematic in some others.

An obvious downside of asymmetric normalization is the loss of the symmetry in the final measure. In the most common applications of normalized mutual information, where labelings are evaluated against a ground truth, an inherently asymmetric situation, the asymmetric measure makes perfect sense, but in other cases the lack of symmetry can be undesirable. Embedding and visualization methods that employ mutual information as a similarity measure, for example, normally demand symmetry [14]. And in cases where one is comparing two candidate labelings directly to one another, rather than to a separate ground truth, then a symmetric measure may be preferable.

Even in this case, however, the asymmetric measure may sometimes be the better choice, as discussed in the introduction. For instance, when one labeling  $c_1$  is a refinement of the other  $c_2$ , the information content is inherently asymmetric:  $c_1$  says more about  $c_2$  than  $c_2$  does about  $c_1$ . An explicit example of this type of asymmetry is shown in Figure 3, where we consider two labelings of 27 objects. The left labeling  $c_1$  is a detailed partition

of the objects into nine small groups while the right labeling  $c_2$  is a coarser partition into only three groups, each of which is an amalgamation of three of the smaller groups in  $c_1$ . Because of this nested relationship, it is relatively easy to transmit  $c_2$  given knowledge of  $c_1$  but more difficult to do the reverse. This imbalance is reflected in the asymmetrically normalized mutual information values in each direction (top and bottom arrows in the figure), but absent from the symmetric version (middle row).

Combining the benefits of asymmetric normalization and the reduced mutual information, we advocate in favor of the asymmetrically-normalized reduced mutual information defined by

$$NMI^{(A)}(c; g) = \frac{I(c; g)}{I(g; g)}, \quad (32)$$

where the mutual information  $I(c; g)$  is quantified as in Eq. (12). This measure correctly accounts for the information contained in the contingency table, returns 0 in expectation when  $c$  is uncorrelated with the ground truth and 1 when  $c = g$ , and always favors the same labeling as the unnormalized measure.

### III. EXAMPLE APPLICATION: COMMUNITY DETECTION

As an example of the performance of the various measures discussed above, we describe in this section the results of an extensive series of tests in which the measures are used to score the output of algorithms for network community detection. In these tests we use the



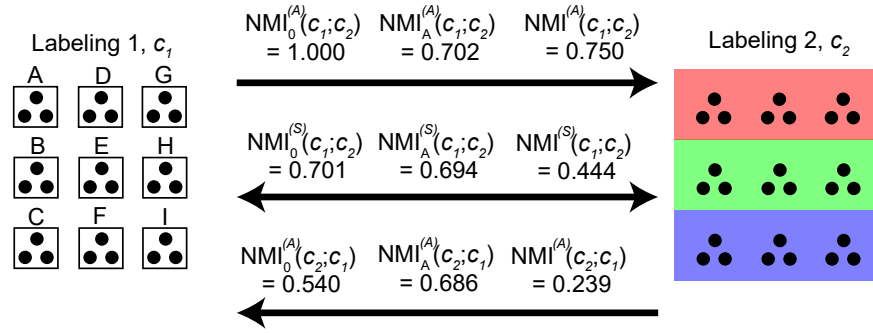


FIG. 3. Values of the various normalized mutual information measures we consider, between two example partitions of the same set of 27 objects. The left partition  $c_1$  divides the objects into nine groups of three objects each and is a refinement of the right partition  $c_2$ , which divides them into only three groups, aggregating those on the left. The arrows indicate the direction of the comparison and the accompanying notations give the values of the mutual information measures. All three asymmetrically normalized measures capture the intuition that the partition  $c_1$  tells us more about  $c_2$  than  $c_2$  tells us about  $c_1$ .

popular Lancichinetti-Fortunato-Radicchi (LFR) graph model [15] to generate random test networks with known community structure and realistic distributions of node degrees and group sizes, and then attempt to recover that structure using a variety of standard community detection algorithms, quantifying the accuracy of the recovery with six different measures: symmetrically normalized versions of the traditional mutual information, the adjusted mutual information, and the reduced mutual information, and asymmetrically normalized versions of the same. A number of studies have been performed in the past to test the efficacy of community detection algorithms on LFR benchmark networks [10–13], but using only the symmetrically normalized, non-reduced mutual information as a similarity measure. Our results indicate that this measure can produce biased outcomes and we recommend the asymmetric reduced mutual information instead.

The LFR model contains a number of free parameters that control the size of the networks generated, their degree distribution, the distribution of community sizes, and the relative probability of within- and between-group edges. (We give further details on the LFR generative process in Appendix A.) We find that the distributions of degrees and community sizes do not significantly impact the relative performance of the various algorithms tested and that performance differences are driven primarily by the size  $n$  of the networks and the mixing parameter  $\mu$  that controls the ratio of within/between-group connections, so our tests focus on performance as a function of these variables.

We perform community detection using six well-known algorithms as follows. (We use the implementations found in the `igraph` library [16], except for the inference method, for which we use the `graph-tool` library [17].)

1. **InfoMap:** InfoMap is an information theoretic approach that defines a compression algorithm for encoding a random walk on a network, based on which communities the walk passes through [18]. Differ-

ent community labelings give rise to more or less efficient compression, as quantified by the so-called map equation, and the labeling with the highest efficiency is considered the best community division.

2. **Modularity maximization:** Modularity is a quality function for network labelings equal to the fraction of edges within communities minus the expected such fraction if edge positions are randomized while preserving the node degrees. The labeling with the highest modularity is considered the best community division. Modularity can be maximized using a number of heuristic methods, of which the most popular are agglomerative methods such as the Louvain and Leiden algorithms [19, 20], spectral methods [21], and simulated annealing [22–24]. In our tests we use simulated annealing where computationally feasible and the Leiden algorithm otherwise, these approaches giving the most consistent maximization of the modularity.
3. **Modularity with a resolution parameter:** Standard modularity maximization is known to suffer from a “resolution limit”—it cannot detect communities smaller than a certain threshold size [25]. This can be remedied using a variant of modularity that includes a resolution parameter  $\gamma$  such that higher values of  $\gamma$  cause the algorithm to prefer smaller communities [24]. Standard modularity maximization corresponds to  $\gamma = 1$ , but for comparison we also conduct tests with  $\gamma = 10$  using the Leiden algorithm.
4. **Statistical inference:** Another popular approach to community detection makes use of model fitting and statistical inference. In this context the most commonly fitted model is the degree-corrected stochastic block model [26], which can be fitted using Bayesian methods to find the best community division [27].



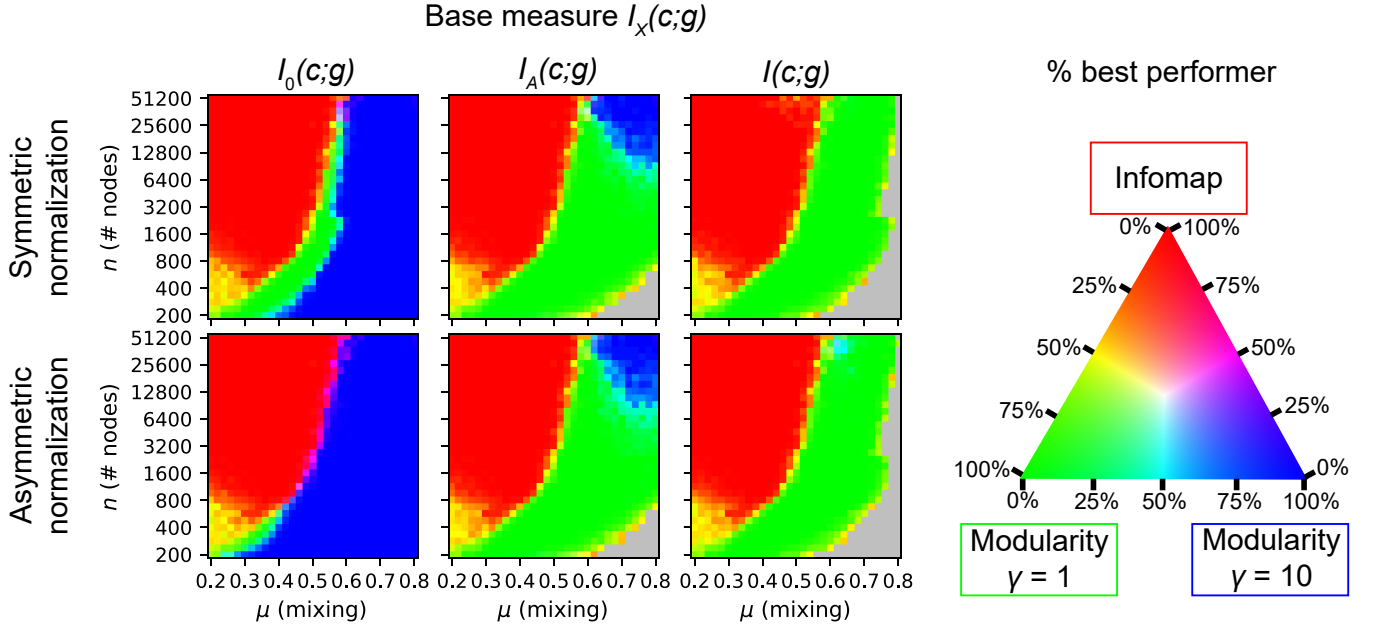


FIG. 4. The colors in each panel in the center of this figure indicate which of three community detection algorithms (InfoMap (red) and modularity maximization with  $\gamma = 1$  (green) and  $\gamma = 10$  (blue)—see key on right) are best able to find the known communities in a large set of LFR benchmark networks, according to the six mutual information measures we consider. Mixtures of red, green, and blue denote the proportions of test cases in which each algorithm performs best. Regions in gray indicate parameter values for which no algorithm achieved a positive mutual information score.

5. **Walktrap:** Walktrap is an agglomerative algorithm in which initially separate nodes are iteratively combined into progressively larger communities in order from strongest to weakest connections, where strength is quantified in terms of the time for a random walk to reach one node from another [28].

6. **Labelprop:** The label propagation or “label-prop” algorithm initially places every node in its own community then iteratively updates the labels of randomly chosen nodes by majority vote among their network neighbors, breaking ties at random [29].

As described in Section III B, all of these algorithms perform reasonably well, but, as we will see, the best performers in the context of the current tests are InfoMap and the two variants of modularity maximization.

#### A. Comparison between variants of the mutual information

Figure 4 summarizes the relative performance of the various mutual information measures in our tests. In this set of tests we limited ourselves, for the sake of clarity, to the top three community detection algorithms—InfoMap and the two variants of modularity maximization—and measured which of the three returned the best results according to each of our six mutual information measures,

as a function of network size  $n$  and the mixing parameter  $\mu$ . Each point in each of the six panels in the figure is color-coded with some mix of red, green, and blue to indicate in what fraction of cases each of the algorithms performs best according to each of the six measures and, as we can see, the results vary significantly among measures. An experimenter trying to choose the best algorithm would come to substantially different conclusions depending on which measure they use.

One consistent feature of all six mutual information measures is the large red area in each panel of Fig. 4, which represents the region in which InfoMap performs best. Regardless of the measure used, InfoMap is the best performer on networks with low mixing parameter (i.e., strong community structure) and relatively large network size. For higher mixing (weaker structure) or smaller network sizes, modularity maximization does better. Which version of modularity is best, however, depends strongly on the mutual information measure. The traditional symmetrically normalized mutual information (top left panel) mostly favors the version with a high resolution parameter of  $\gamma = 10$  (blue), but the asymmetric reduced measure for which we advocate (bottom right) favors the version with  $\gamma = 1$  (green). (The regions colored gray in the figure are those in which no algorithm receives a positive mutual information score and hence all algorithms can be interpreted as failing.)

These results raise significant doubts about the traditional measure. At large  $n$  and high mixing  $\mu$  the network will have many small communities, and in this

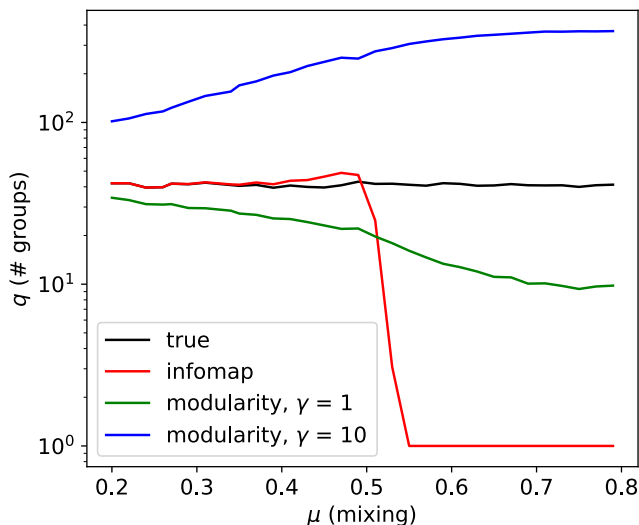


FIG. 5. The number of groups inferred by each of the six algorithms in Fig. 4 for LFR benchmark networks with  $n = 3200$  nodes and a range of values of the mixing parameter  $\mu$ . The true number of groups is shown in black. The InfoMap algorithm (red) generates an accurate number of groups for values of  $\mu$  up to about 0.5, but beyond this point it erroneously places all nodes in a single group. Standard modularity maximization with resolution parameter  $\gamma = 1$  (green) underestimates the number of groups, presumably because of the resolution limit on the detection of small groups, but not as severely as the number is overestimated when  $\gamma = 10$  (blue).

regime it is natural that modularity maximization with a high resolution parameter will perform well because it favors large numbers of communities, and all mutual information measures agree on this point. For smaller system sizes or lower mixing, however, the network will have fewer, larger communities and in this regime we find that the  $\gamma = 10$  algorithm dramatically overestimates the number of communities in the network. With a non-reduced mutual information there is no penalty for doing this, as discussed in Section II A, which is why the traditional normalized mutual information ranks the  $\gamma = 10$  algorithm highly in this regime, arguably erroneously. The reduced mutual information, by contrast, prefers the  $\gamma = 1$  algorithm. The number of groups inferred by each algorithm for each value of the mixing parameter  $\mu$  is shown for  $n = 3200$  in Figure 5, which highlights these findings.

An extreme example of the disagreement between measures can be seen in the lower right corner of each plot in Fig. 4, where most measures return a negative value, indicating that community detection has failed altogether. This is expected: for very weak community structure all detection algorithms are expected to show a “detectability threshold” beyond which they are unable to identify any communities [30–32]. The standard normalized mutual information, however, claims to find community structure in this regime using the  $\gamma = 10$  version of mod-

ularity maximization. This occurs because the  $\gamma = 10$  algorithm finds many small communities and, as discussed in Section II A, a labeling with many communities, even completely random ones, is accorded a high score by a non-reduced mutual information. This offers a clear reason to avoid the standard measure.

The bottom left panel in Fig. 4 shows results for the asymmetrically normalized version of the traditional mutual information, which gives even worse results than the symmetric version, with hardly any region in which the  $\gamma = 1$  version of modularity maximization outperforms the  $\gamma = 10$  version. This behavior arises for the reasons discussed in Section II B: the bias inherent in the symmetric normalization fortuitously acts to partially correct the errors introduced by neglecting the information content of the contingency table. The asymmetric normalization eliminates this correction and hence performs more poorly. The correct solution to this problem, however, is not to use a symmetric normalization, which can bias outcomes in other ways as we have seen, but rather to adopt a reduced mutual information measure.

Finally, comparing the middle and right-hand columns of Fig. 4, we see that the results for the adjusted and reduced mutual information measures are quite similar in these tests, although there are some differences. In particular, the adjusted measure appears to find more significant structure for higher mixing than the reduced measure. This occurs because, as discussed in Section II A and Ref. [6], the adjusted measure encodes the contingency table in a way that is optimized for more uniform tables than the reduced measure, and thus penalizes uniform tables less severely, leading to overestimates of the mutual information in the regime where detection fails—in this regime the candidate and ground-truth labelings are uncorrelated which results in a uniform contingency table. This provides further evidence in favor of using a reduced mutual information measure.

## B. Comparison between community detection algorithms

Settling on the asymmetrically normalized reduced mutual information as our preferred measure of similarity, we now ask which community detection algorithm or algorithms perform best according to this measure? We have already given away the answer—InfoMap and modularity maximization get the nod—but here we give evidence for that conclusion.

Figure 6 shows results for all six algorithms listed in Section III. Examining the figure, we see that in general the best-performing methods are InfoMap, traditional modularity maximization with  $\gamma = 1$ , and the inference method using the degree-corrected stochastic block model. Among the algorithms considered, InfoMap achieves the highest mutual information scores for lower values of the mixing parameter  $\mu$  in the LFR model, but fails abruptly as  $\mu$  increases, so that beyond a fairly sharp

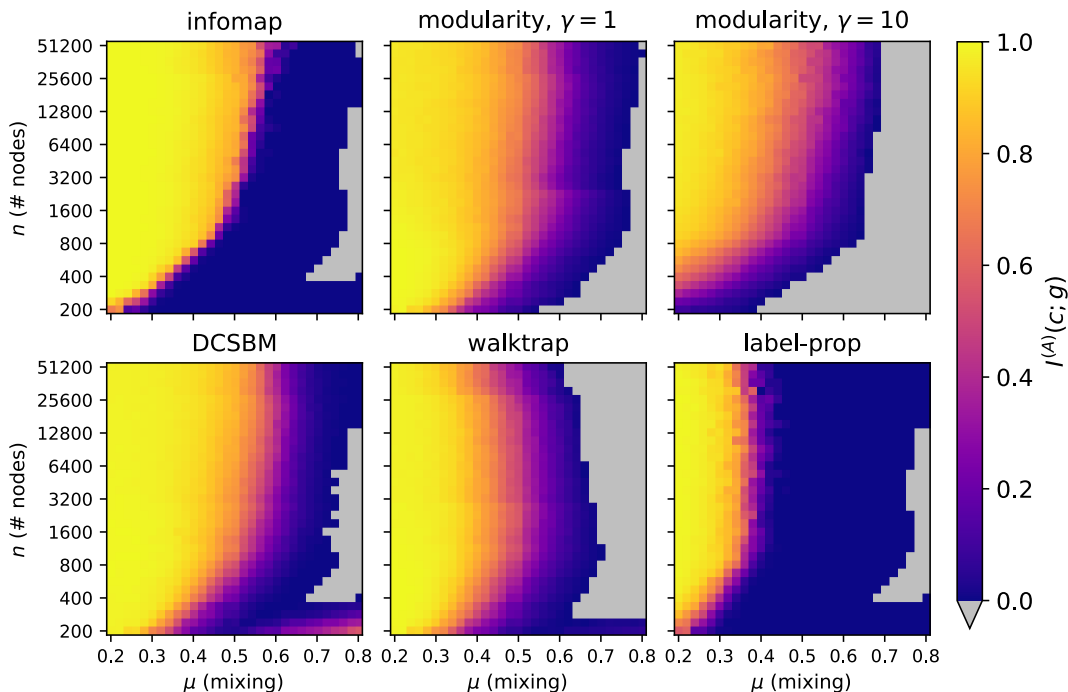


FIG. 6. Performance of each of the six community detection algorithms considered here in identifying the known communities in a large set of LFR benchmark networks, as quantified by the asymmetrically normalized reduced information measure  $I^{(A)}(c; g)$  proposed in this paper.

cutoff around  $\mu = 0.5$  other algorithms do better. As noted by previous authors [33], InfoMap’s specific failure mode is that it places all nodes in a single community and this behavior can be used as a simple indicator of the failure regime. In this regime one must use another algorithm. Either modularity maximization or inference using the degree-corrected stochastic block model are reasonable options, but modularity has a slight edge, except in a thin band of intermediate  $\mu$  values which, in the interests of simplicity, we choose to ignore. (We discuss some caveats regarding the relationship between the degree-corrected stochastic block model and the LFR benchmark in Appendix A.)

Thus our recommendations for the best community detection algorithm are relatively straightforward, if we base our choice on performance under the LFR benchmark, as is commonly done in this field. If we are in a regime where InfoMap succeeds, meaning it finds more than one community, then one should use InfoMap. If not, one should use standard modularity maximization with  $\gamma = 1$ . That still leaves open the question of how the modularity should be maximized. In our studies we find the best results with simulated annealing, but simulated annealing is computationally expensive. In regimes where it is not feasible, we recommend using the Leiden algorithm instead. (Tests using other computationally efficient maximization schemes, such as the Louvain and spectral algorithms, generally performed less well than the Leiden algorithm.)

#### IV. CONCLUSIONS

In this paper we have examined the performance of a range of mutual information measures for comparing labelings of objects in classification, clustering, or community detection applications. We argue that the commonly used normalized mutual information is biased in two ways: (1) because it ignores the information content of the contingency table, which can be large, and (2) because the symmetric normalization it employs introduces spurious dependence on the labeling. We argue in favor of a different measure, an asymmetrically normalized version of the so-called reduced mutual information, which rectifies both of these shortcomings.

To demonstrate the effects of using different mutual information measures, we have presented results of an extensive set of numerical tests on popular network community detection algorithms, as evaluated by the various measures we consider. We find that conclusions about which algorithms are best depend substantially on which measure we use.

#### ACKNOWLEDGMENTS

The authors thank Samin Aref for useful comments and feedback. This work was supported in part by the US National Science Foundation under grants DMS-2005899 and DMS-2404617, and by computational resources pro-

vided by the Advanced Research Computing initiative at the University of Michigan.

## Appendix A: Benchmarking

In this appendix we give some additional details of our numerical tests.

### 1. Results for the traditional symmetric normalized mutual information

Figure 7 shows the performance of the same six community detection methods as in Fig. 6, but measured using the standard, symmetrically normalized, non-reduced mutual information  $I_0^{(S)}(c; g)$ . By this measure many of the methods appear to perform implausibly well, far beyond the detectability threshold visible in Fig. 6 in the regime where all methods should by rights fail. Note in particular the high scores achieved by the generalized modularity with  $\gamma = 10$  in this undetectable regime by virtue of the excessive number of groups it generates.

### 2. LFR network generation

The LFR networks we use for benchmarking are generated using the procedure described in [15], which is as follows.

1. **Fix the number of nodes  $n$  and mixing parameter  $\mu$ .** In our studies we use node counts in the range  $n \in [200, 51200]$ . The parameter  $\mu$  controls the relative number of edges within and between communities. For small  $\mu$  there are many more edges within communities than between them, which makes the communities relatively easy to detect. But as  $\mu$  gets larger there are more edges between communities and detection becomes more difficult in a manner reminiscent of the detectability threshold in the standard stochastic block model [30, 34]. In our studies we use values of  $\mu$  in the range  $[0.2, 0.8]$ .
2. **Draw a degree sequence** from a power-law distribution with exponent  $\tau_1$ . Many networks have power-law degree distributions, typically with exponents between 2 and 3 [35], and the LFR model exclusively uses power-law distributions. We use  $\tau_1 = 2.5$ , with average degree  $\langle k \rangle = 20$  and maximum degree (which depends on graph size)  $k_{\max} = n/10$ . Empirically, however, our results do not seem to be very sensitive to these choices.
3. **Draw a set of community sizes** from a power-law distribution with exponent  $\tau_2$ . Many networks

are also found to have community sizes that approximately follow a power law, with typical exponents in the range from 1 to 2 [15, 36–38]. We use  $\tau_2 = 1.5$  with a minimum community size of  $s_{\min} = 20$  in all cases, while the maximum community size is set to  $s_{\max} = \max\{n/10, 100\}$ . Again, results were not particularly sensitive to these choices, provided they produce a valid distribution at all.

4. **Assign each node to a community** randomly, one node at a time, while ensuring that the community chosen is always large enough to support the added node’s intra-community degree, given by  $(1 - \mu)k$  where  $k$  is the total degree.
5. **Rewire the edges** attached to each node while preserving the node degrees, until the fraction of edges running between nodes in different communities is approximately  $\mu$ .

The parameter values above are similar to those used for instance in [12]. As in that study, we find that algorithm performance is dictated primarily by the parameters  $n$  and  $\mu$ , so it is these parameters that are varied our summary figures.

The LFR model is similar to a special case of the degree-corrected stochastic block model (DCSBM) [26], and hence one might expect that inference-based community detection methods employing the latter model would perform optimally on LFR networks. Specifically, in the limit of an infinite number of sampled networks and perfect optimization of each community detection method, the final performance measure for any algorithm is given by the expectation value of the similarity  $M(g, h[A])$  between the ground truth LFR partition  $g$  and the partition  $h[A]$  of the LFR network  $A$  inferred using the algorithm, where the expectation is taken over the ensemble  $P(A, g|\theta)$  of LFR networks and partitions  $A, g$  generated using parameters  $\theta$  (meaning  $\mu, \tau_1, \tau_2$ , etc.). By using the LFR benchmark with parameters  $\theta$  to compare the performance of community detection algorithms, we are therefore implicitly defining the “best” algorithm to be the one whose corresponding function  $h[A]$  optimizes  $\sum_{A, g} P(A, g|\theta) M(g, h[A])$ . If the similarity measure we choose is the “all or nothing” error function  $M(g, c) = \delta(g, c)$ , then the optimal community detection algorithm is trivially the one with

$$h[A] = \operatorname{argmax}_g P(A, g|\theta) = \operatorname{argmax}_g P(g|A, \theta). \quad (\text{A1})$$

In other words, the optimal algorithm simply performs maximum a posteriori estimation under the model from which the network was generated. There is no explicit formula for the posterior probability under the LFR model, but to the extent that it is a special case of the DCSBM, we might expect the DCSBM (with appropriate priors) to give optimal results [39]. The LFR model, however, is not precisely a special case of the DCSBM. In

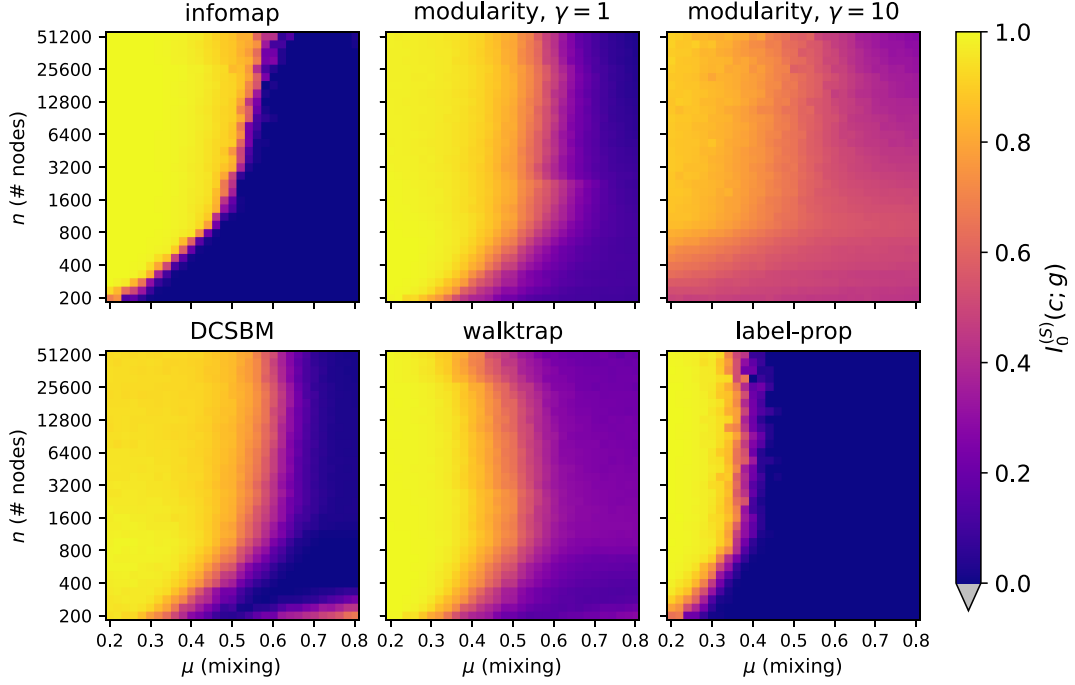


FIG. 7. Performance of each of the six community detection algorithms considered here, as quantified by the conventional symmetrically normalized, non-reduced mutual information  $I_0^{(S)}(c; g)$ .

particular, the DCSBM normally assumes a uniform distribution over community sizes, where the LFR model assumes a power law. Moreover, we are not using the crude all-or-nothing error function: our entire purpose in this paper is to develop mutual information measures that aggregate and weigh different modes of error in a sensible fashion. These differences, it appears, are enough to ensure that the DCSBM does not perform the best in our testing.

Regardless, we emphasize that our use of the LFR benchmark in our analysis is simply for consistency with previous studies of network community detection methods [10, 12, 15]. The justification for our proposed similarity measure, on the other hand, is chiefly its theoretical merit over the conventional (symmetric, non-reduced) normalized mutual information, and is independent of the use of the LFR (or any other) benchmark.

- 
- [1] T. M. Cover and J. A. Thomas, *Elements of Information Theory*. John Wiley, New York, 2nd edition (2006).
  - [2] L. Danon, J. Duch, A. Diaz-Guilera, and A. Arenas, Comparing community structure identification. *J. Stat. Mech.* **2005**, P09008 (2005).
  - [3] A. Amelio and C. Pizzuti, Correction for closeness: Adjusting normalized mutual information measure for clustering comparison. *Computational Intelligence* **33**(3), 579–601 (2017), URL <https://onlinelibrary.wiley.com/doi/abs/10.1111/coin.12100>.
  - [4] N. X. Vinh, J. Epps, and J. Bailey, Information theoretic measures for clusterings comparison: Variants, properties, normalization and correction for chance. *Journal of Machine Learning Research* **11**, 2837–2854 (2010).
  - [5] A. J. Gates and Y.-Y. Ahn, The impact of random models on clustering similarity. Preprint arXiv:1701.06508 (2017).
  - [6] M. E. J. Newman, G. T. Cantwell, and J.-G. Young, Improved mutual information measure for clustering, classification, and community detection. *Phys. Rev. E* **101**, 042304 (2020).
  - [7] M. Jerdee, A. Kirkley, and M. Newman, Mutual information and the encoding of contingency tables. *arXiv:2405.05393* (2024).
  - [8] L. Ana and A. Jain, Robust data clustering. In *2003 IEEE Computer Society Conference on Computer Vision and Pattern Recognition, 2003. Proceedings.*, volume 2, pp. II–II (2003).
  - [9] P. Zhang, Evaluating accuracy of community detection using the relative normalized mutual information. *J. Stat. Mech.* **2015**, P11006 (2015).
  - [10] A. Lancichinetti and S. Fortunato, Community detection algorithms: A comparative analysis. *Phys. Rev. E* **80**, 056117 (2009).
  - [11] G. K. Orman, V. Labatut, and H. Cherifi, Qualitative comparison of community detection algorithms. *Communications in Computer and Information Science* **167**, 265–279 (2011).
  - [12] Z. Yang, R. Algesheimer, and C. J. Tessone, A comparative analysis of community detection algorithms on ar-

- tificial networks. *Scientific Reports* **6**, 30750 (2016).
- [13] S. Fortunato and D. Hric, Community detection in networks: A user guide. *Physics Reports* **659**, 1–44 (2016).
  - [14] L. Peel, D. B. Larremore, and A. Clauset, The ground truth about metadata and community detection in networks. *Science Advances* **3**, e1602548 (2017).
  - [15] A. Lancichinetti, S. Fortunato, and F. Radicchi, Benchmark graphs for testing community detection algorithms. *Phys. Rev. E* **78**, 046110 (2008).
  - [16] G. Csardi and T. Nepusz, The igraph software package for complex network research. *InterJournal Complex Systems*, 1695 (2006), URL <https://igraph.org>.
  - [17] T. P. Peixoto, The graph-tool python library. *figshare* (2014), URL [http://figshare.com/articles/graph\\_tool/1164194](http://figshare.com/articles/graph_tool/1164194).
  - [18] M. Rosvall and C. T. Bergstrom, Maps of random walks on complex networks reveal community structure. *Proc. Natl. Acad. Sci. USA* **105**, 1118–1123 (2008).
  - [19] V. D. Blondel, J.-L. Guillaume, R. Lambiotte, and E. Lefebvre, Fast unfolding of communities in large networks. *J. Stat. Mech.* **2008**, P10008 (2008).
  - [20] V. A. Traag, L. Waltman, and N. J. Van Eck, From louvain to leiden: guaranteeing well-connected communities. *Scientific reports* **9**, 5233 (2019).
  - [21] M. E. J. Newman, Modularity and community structure in networks. *Proc. Natl. Acad. Sci. USA* **103**, 8577–8582 (2006).
  - [22] R. Guimerà, M. Sales-Pardo, and L. A. N. Amaral, Modularity from fluctuations in random graphs and complex networks. *Phys. Rev. E* **70**, 025101 (2004).
  - [23] A. Medus, G. Acuña, and C. O. Dorso, Detection of community structures in networks via global optimization. *Physica A* **358**, 593–604 (2005).
  - [24] J. Reichardt and S. Bornholdt, Statistical mechanics of community detection. *Phys. Rev. E* **74**, 016110 (2006).
  - [25] S. Fortunato and M. Barthélemy, Resolution limit in community detection. *Proc. Natl. Acad. Sci. USA* **104**, 36–41 (2007).
  - [26] B. Karrer and M. E. J. Newman, Stochastic blockmodels and community structure in networks. *Phys. Rev. E* **83**, 016107 (2011).
  - [27] T. P. Peixoto, Nonparametric Bayesian inference of the microcanonical stochastic block model. *Phys. Rev. E* **95**, 012317 (2017).
  - [28] P. Pons and M. Latapy, Computing communities in large networks using random walks. In P. Yolum, T. Güngör, F. S. Gürgeç, and C. C. Özturan (eds.), *Proceedings of the 20th International Symposium on Computer and Information Sciences*, volume 3733 of *Lecture Notes in Computer Science*, pp. 284–293, Springer, New York (2005).
  - [29] U. N. Raghavan, R. Albert, and S. Kumara, Near linear time algorithm to detect community structures in large-scale networks. *Phys. Rev. E* **76**, 036106 (2007).
  - [30] A. Decelle, F. Krzakala, C. Moore, and L. Zdeborová, Inference and phase transitions in the detection of modules in sparse networks. *Phys. Rev. Lett.* **107**, 065701 (2011).
  - [31] L. Massoulié, Community detection thresholds and the weak Ramanujan property. In *Proceedings of the 46th Annual ACM Symposium on the Theory of Computing*, pp. 694–703, Association of Computing Machinery, New York (2014).
  - [32] E. Mossel, J. Neeman, and A. Sly, Reconstruction and estimation in the planted partition model. *Probability Theory and Related Fields* **162**, 431–461 (2015).
  - [33] S. Aref, H. Chheda, and M. Mostajabdaveh, The Bayan algorithm: Detecting communities in networks through exact and approximate optimization of modularity. Preprint arXiv:2209.04562 (2022).
  - [34] A. Decelle, F. Krzakala, C. Moore, and L. Zdeborová, Asymptotic analysis of the stochastic block model for modular networks and its algorithmic applications. *Phys. Rev. E* **84**, 066106 (2011).
  - [35] G. Caldarelli, *Scale-Free Networks*. Oxford University Press, Oxford (2007).
  - [36] R. Guimerà, L. Danon, A. Díaz-Guilera, F. Giralt, and A. Arenas, Self-similar community structure in a network of human interactions. *Phys. Rev. E* **68**, 065103 (2003).
  - [37] A. Clauset, M. E. J. Newman, and C. Moore, Finding community structure in very large networks. *Phys. Rev. E* **70**, 066111 (2004).
  - [38] G. Palla, I. Derényi, I. Farkas, and T. Vicsek, Uncovering the overlapping community structure of complex networks in nature and society. *Nature* **435**, 814–818 (2005).
  - [39] T. P. Peixoto, Revealing consensus and dissensus between network partitions. *Physical Review X* **11**, 021003 (2021).